

ACCURACY OF HETEROGENEOUS STAGGERED-GRID FINITE-DIFFERENCE MODELING OF RAYLEIGH WAVES

T. Bohlen and E.H. Saenger

email: saenger@geophysik.fu-berlin.de

keywords: finite-difference modeling, Rayleigh waves, accuracy

ABSTRACT

Heterogenous Finite-Difference (FD) modeling assumes that the boundary conditions of the elastic wavefield between material discontinuities are implicitly fulfilled by the distribution of the elastic parameters on the numerical grid. It is widely applied to weak elastic contrasts between geological formations inside the earth. In this work we test the accuracy at the free surface of the earth. The accuracy for modeling Rayleigh waves using the conventional standard staggered-grid (SSG) and the rotated staggered grid (RSG) is investigated. The accuracy tests reveal that one cannot rely on conventional numerical dispersion discretization criteria. A significant higher sampling is necessary to obtain acceptable accuracy. In case of planar free surfaces aligned with the grid, 15 to 30 grid points per minimum wavelength of the Rayleigh wave are required. The widely used explicit boundary condition, the so-called image method, produces similar accuracy and requires approximately half the sampling of the wavefield compared to heterogeneous free surface modelling. For a free surface not aligned with the grid (surface topography) the error increases significantly and varies with the dip angle of the interface. For an irregular interface the RSG scheme is more accurate than the SSG scheme. The RSG scheme, however, requires 60 grid points per minimum wavelength to achieve good accuracy for all dip angles. The high computation requirements for 3-D simulations on such fine grids limit the application of heterogenous modeling in the presence of complex surface topography.

INTRODUCTION

Accurate simulation of seismic waves in heterogeneous models containing strong contrast discontinuities with 3-D topography is an important capability for solving a wide variety of seismic modeling problems ranging from earthquake site studies to environmental or engineering applications. A popular method for the computation of synthetic seismograms is to use regular grid Finite-Difference (FD) algorithms. One main advantage of the FD method is that it can be applied to fairly complex models. Two approaches are used to fulfill the physical boundary conditions between two media: the homogeneous and heterogeneous approach.

In the homogeneous approach the equations of motion are combined with explicit traction continuity conditions at interfaces. This approach is often applied at free surfaces. For instance, a popular, simple and stable method is the imaging method, where stress fields are imaged as odd functions across a free surface (Levander, 1988; Graves, 1996; Robertsson, 1996; Robertsson and Holliger, 1997; Gottschämer and Olsen, 2001; Imhof, 2003). However, numerical difficulties for modeling free surfaces may occur (Hestholm, 2003; Gottschämer and Olsen, 2001). Other algorithms have been proposed in which the grid coordinates are rotated parallel to the inclined boundary (Jih et al., 1988) or in which the grid is deformed to be able to match the boundary conditions at free surfaces with 3-D topography (Fornberg, 1988; Hestholm and Ruud, 1998; Tessmer and Kosloff, 1994).

In the heterogeneous approach the boundary conditions are assumed to be implicitly fulfilled by the distribution of elastic parameters on the grid. Boundary conditions across discontinuities are not treated

explicitly. This approach was introduced e.g. by Boore (1972) and Kelly et al. (1976), and was more recently mathematically justified by Zahradník and Priolo (1999) and Moczo et al. (2002). The same FD formulas are used everywhere, also across free surfaces. The material parameters are represented by their actual local values or by arithmetic or harmonic averages from neighboring grid points. For instance, to realize a free surface the Lamé parameters above the surface can be set to zero and the density close to zero (to avoid division by zero) to approximate a vacuum. This procedure is also referred to as the "vacuum formalism" (Zahradník et al., 1993). Heterogeneous modeling of free surfaces thus implies the application of the vacuum formalism. Therefore both terms are used synonymously throughout this paper.

The heterogeneous approach is obviously very attractive because of its simplicity and high flexibility compared to the other explicit methods mentioned above. Complex shaped strong contrast discontinuities can be simulated with the same algorithm. All that is required is to change the distribution of the elastic parameters in the computational region depending on the free surface topography under consideration.

Some examples for the application of the vacuum formalism exist in the literature. Frankel and Leith (1992) successfully simulated free surface topography with an FD scheme of fourth-order accuracy in space using a variation of the vacuum formalism. They use a density taper to zero starting at the free surface while keeping the medium P-velocity unaltered. Unfortunately, their method was not thoroughly bench-marked. Zahradník and Urban (1984) applied the vacuum formalism to SH-waves at curved free surfaces and found good agreement with an independent solution. Zahradník et al. (1993) used the vacuum formalism in four different 2-D P-SV finite difference schemes and investigated their behavior at a planar free surface which is aligned with the grid. Their numerical results are in qualitative agreement with semi-analytic solutions even for a method that theoretically does not fulfill the traction condition. Zahradník et al. (1993) used 5 grid points per wavelength for a 4th-order scheme and 10 gridpoints per wavelength for the 2nd-order algorithms. Unfortunately, they did not analyze the performance for different grid spacings. Ohminato and Chouet (1997) also apply the vacuum formalism in a 3-D scheme in which the shear stresses are distributed on the 12 edges of the FD cell so that only shear stresses appear on the free surface and normal stresses remain embedded within the solid region. Numerical tests indicate that 25 grids per wavelength are required to obtain sufficient accuracy. Opršal and Zahradník (1999) propose an elastic 2-D FD method for spatially irregular grids on which the vacuum formalism is applied to implement free surfaces. For a horizontal free surface they tested the accuracy for grid spacings of 13 and 27 grid points per minimum wavelength. They discovered sufficient accuracy for the Rayleigh wave. Saenger et al. (2000) suggested the use of a rotated staggered grid finite difference scheme in which the spatial derivatives are rotated by 45 degrees which leads to a partly staggered distribution of wavefield and material parameters that is well suited for the vacuum formalism. The accuracy of this approach has been successfully verified for modeling SH-wave scattering at a cavity by comparison with an analytical solution (Krüger et al., 2005). Krüger et al. (2005) found sufficient accuracy for 30 grid points and good accuracy for 300 grid points per minimum wavelength. The results of the modeling of Rayleigh waves propagating along the 3-D topography of a hill computed with the RSG agree well with results obtained by Ohminato and Chouet (1997) for the same geological model (Saenger and Bohlen, 2004). Graves (1996) applied the vacuum formalism on the standard staggered grid (Virieux, 1986; Levander, 1988) and simulated Rayleigh waves propagating along a horizontal free surface aligned with the grid. He used 9 grid points per minimum wavelength and found a not very satisfying agreement with a frequency-wavenumber technique. More recently, Hayashi et al. (2001) concluded that at least 30 grid points per minimum wavelength are required for modelling Rayleigh waves on free surfaces with topography using the vacuum method on a standard staggered grid. Their accuracy tests are based on convergence tests.

In this paper we explore the performance of two different viscoelastic velocity-stress 2-D FD algorithms, namely (1) the widely used standard staggered grid (SSG) (Virieux, 1986; Levander, 1988; Robertson et al., 1994; Graves, 1996; Bohlen, 2002) and (2) the more recently developed rotated staggered grid (RSG) (Gold et al., 1997; Saenger et al., 2000; Saenger and Bohlen, 2004). A goal of this work is to establish relations between desired accuracy and computational costs. How finely must the wavefield be sampled to achieve acceptable results? Is heterogeneous modeling of free surfaces a reasonable alternative to using explicit boundary conditions? As a critical test, we perform modeling of Rayleigh waves propagating along planar free surfaces having different orientations with respect to the grid.

We proceed with a short description of the location of wavefield parameters and material properties on the standard and rotated staggered grid. The correct averaging of material parameters is described. The

results of the accuracy tests are presented subsequently.

STANDARD AND ROTATED STAGGERED GRID

Figure 1 shows a comparison of the locations of viscoelastic wavefield parameters and material parameters on the standard staggered grid (SSG) and the rotated staggered grid (RSG).

On the SSG, different components of one physical parameter are defined at different staggered points. For example, the two different components of the particle velocity (circles in Figure 1a) are distributed over two different staggered locations. The different components of the stress tensor (indicated by squares in Figure 1a) are distributed over two different locations. The shear modulus μ and the S-wave attenuation parameter τ^s Blanch et al. (1995); Bohlen (2002) are required at the locations of shear-stress components. The density ρ is required at the locations of particle velocities. These material parameters thus need to be locally averaged, i.e. calculated from neighboring grid points. The averaging of material parameters is critical for the accuracy at strong discontinuities (Zahradník et al., 1993; Falk, 1998; Moczo et al., 2002). To obtain stable results, arithmetic averaging must be used for the density ρ and attenuation parameter τ^s , and harmonic averaging is required for the shear modulus (Fellinger et al., 1995; Graves, 1996; Falk, 1998; Vossen et al., 2002; Moczo et al., 2002):

$$\begin{aligned}
 \rho_x(i+1/2, j) &= \frac{\rho(i, j) + \rho(i+1, j)}{2}, \\
 \rho_y(i, j+1/2) &= \frac{\rho(i, j) + \rho(i, j+1)}{2}, \\
 \tau_{xy}^s(i+1/2, j+1/2) &= \frac{\tau^s(i, j) + \tau^s(i+1, j) + \tau^s(i+1, j+1) + \tau^s(i, j+1)}{4}, \\
 \mu_{xy}(i+1/2, j+1/2) &= \frac{4}{\mu^{-1}(i, j) + \mu^{-1}(i+1, j) + \mu^{-1}(i+1, j+1) + \mu^{-1}(i, j+1)}.
 \end{aligned} \tag{1}$$

This averaging procedure satisfies the condition of traction continuity across the interface between two media on standard staggered grids Moczo et al. (2002). Our numerical tests show that arithmetic averaging of the shear modulus across free surfaces leads to instabilities. Harmonic averaging produces stable simulations. For the SSG the location of the free surface is defined by the plane going through the staggered position of the particle velocity v_y and shear stress σ_{xy} (Figure 1a).

In the case of the RSG, all stress tensor components are located at one (full) grid point and all particle velocities are located at one staggered point (Figure 1b). This partly staggered distribution of wavefield and material parameters is obtained by the rotation of the derivatives direction (Gold et al., 1997; Saenger et al., 2000). In the case of the RSG only densities need to be arithmetically averaged (Figure 1b):

$$\bar{\rho}(i+1/2, j+1/2) = \frac{1}{4} \{ \rho(i, j) + \rho(i+1, j) + \rho(i+1, j+1) + \rho(i, j+1) \} \tag{2}$$

No averaging of the elastic moduli is necessary. This is, among other things, advantageous for the simulation of anisotropic media (Saenger and Bohlen, 2004). Numerical tests show that RSG simulations are stable near vacuum-solid discontinuities, i.e., free surfaces. For the RSG the location of the free surface is defined by the plane going through the staggered position of the particle velocities (Figure 1b).

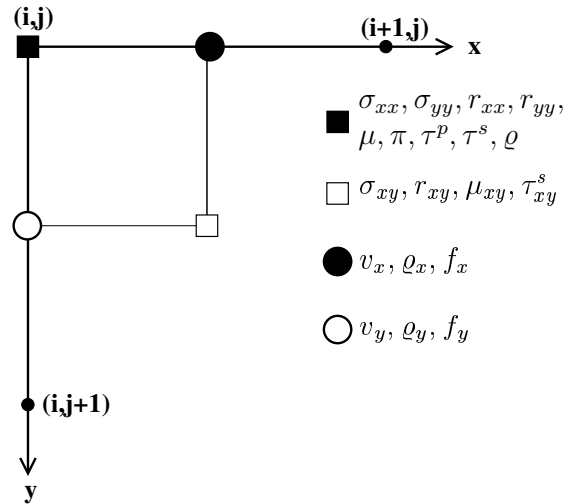
For both schemes we apply second order spatial FD operators (O(2,2)) only. The application of higher-order spatial FD operators is not reasonable due to the discontinuities of the seismic wavefield at the free surface (Cunha, 1993).

ACCURACY TESTS

Planar free surface aligned with the grid

First we evaluate the performance of both schemes for a planar free surface aligned with the numerical grid. Seismic waves are excited by a vertical point force that is applied at a single grid node 0.4 m below the free surface. Receivers are located at the same depth every 1m up to an offset of 60 m. We test the accuracy of Rayleigh waves in two types of half-spaces: (1) a crystalline hard rock and (2) a sedimentary soft rock.

a) Standard Staggered Grid (SSG)



b) Rotated Staggered Grid (RSG)

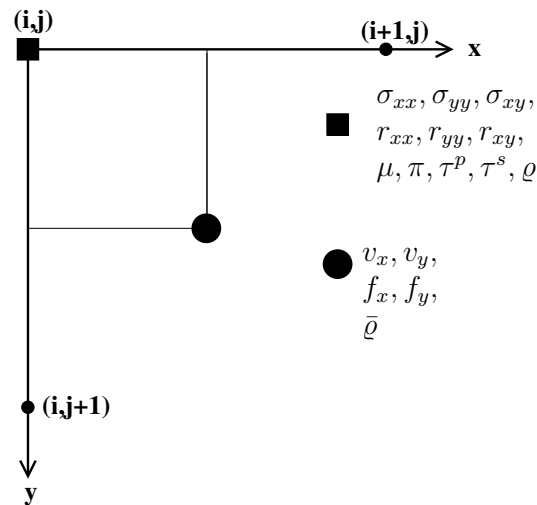


Figure 1: Locations of wavefield and material parameters in a 2-D finite-difference cell for the Standard Staggered Grid (SSG) Virieux (1986); Levander (1988); Robertsson et al. (1994) and the Rotated Staggered Grid (RSG) Saenger et al. (2000). σ_{ij} denote stress components, r_{ij} are the memory variables, v_i are the particle velocities, f_i are the body force components, π is the P-wave modulus, μ is the shear modulus, ρ denotes density, and τ^p and τ^s are the attenuation parameters for P- and S-waves, respectively. μ_{xy} , and τ_{xy}^s , and $\rho_x, \rho_y, \bar{\rho}$ denote averaged material properties for shear modulus, attenuation parameter τ^s , and density, respectively (equations 1 and 2).

The P-velocity, S-velocity, and density of the hard rock half-space are $V_p=5.7$ km/s, $V_s=3.4$ km/s, and $\rho=2200$ kg/m³, respectively. The source signal is a Ricker wavelet with a center frequency of 500 Hz and a maximum frequency of 1.1 kHz. The P-velocity, S-velocity, and density of the soft sediment are $V_p=1.7$ km/s, $V_s=0.17$ km/s, and $\rho=1700$ kg/m³, respectively. This case simulates water saturated sand with a high Poisson ratio of 0.49. In the soft rock simulations we use a Ricker signal with a center frequency of 50 Hz and a maximum frequency of approximately 90 Hz to simulate a hammer blow on the free surface. In both models the grid points above the planar free surface are assigned with zero velocities, and low density (0.00125 kg/m³). In case of the SSG S-velocities are set close to zero to avoid division by zero during harmonic averaging of the shear modulus (equation 1).

The parameters for the spatial and temporal discretization of the two models are listed in Table 1. As a measure of the spatial discretization of the Rayleigh wave we use the number of grid points per minimum wavelength λ_{min}/dh where λ_{min} is determined by the lowest Rayleigh wave velocity and the maximum source frequency $\lambda_{min} = c_{min}/f_{max}$. The time step interval dt is chosen just below the stability limit of the SSG scheme $dt < dh/(\sqrt{2}c_{max})$ Virieux (1986); Blanch et al. (1995) where c_{max} denotes the maximum P-wave velocity. Although the stability criterion of the RSG scheme is less strict ($dt < dh/c_{max}$) (Saenger et al., 2000), we use the same time step dt for both algorithms. Due to the high V_p/V_s ratio of the soft rock, the simulations of the soft rock model require larger run times (Table 1).

The FD modeled waveforms are compared with an analytical solution which uses the Cagniard-De Hoop technique to calculate the Green's function for the elastic halfspace with a free surface (Berg et al., 1994). In order to quantify the relative difference between FD seismograms $f(l\Delta t)$ and the analytical solution $q(l\Delta t)$ we calculate the L2 norm error:

$$E = \frac{\sum_i^N (f(l\Delta t) - q(l\Delta t))^2}{\sum_i^N q(l\Delta t)^2}, \quad (3)$$

where the summation is over the Rayleigh wave event only. A disadvantage of this error measure is that it is particularly sensitive to time shifts rather than amplitude differences when the waveform is distorted. For this reason, waveforms are also compared directly.

Figure 2 shows seismograms of the radial and vertical component of particle velocity for the hard and soft rock case.

Seismograms are recorded at an offset of 60 m corresponding to approximately 40 and 20 times the dominant wavelength of the Rayleigh wave for the soft and hard rock case, respectively. The RSG and SSG algorithms produce nearly identical seismograms for both models. There are two reasons for this: (1) the effective free surface in both schemes is located at the same depth, and (2) parallel to the grid axes the dispersion error for the same time step dt and grid spacing dh is identical (Saenger et al., 2000). Because of the similarity, only the SSG solution is shown. Similar performances of different FD techniques at planar free surfaces aligned with the grid are also reported by Zahradník et al. (1993). For small grid spacing corresponding to more than 17 grid points per minimum wavelength we observe good agreement between the analytical solution and the SSG/RSG seismograms for both models. On coarser grids (9 grid points per minimum wavelength), however, waveforms change significantly with offset. The Rayleigh wave is delayed and ringing after the main event is observed at greater offsets.

The relative errors of the SSG and RSG seismograms are calculated via equation 3 at different offsets. The results are shown in Figure 3.

The error E defined in equation 3 is increasing with offset if the model is discretized with 17 grid points, whereas for 34 grid points the error remains well below 10 %. From this and other numerical tests we conclude that at least 30 grid points are required to obtain accurate results for Rayleigh waves at greater offsets, i.e. more than 40 S-wavelengths at the surface. 15 grid points per minimum wavelength are sufficient for smaller offsets. Fewer grid points are required for the accurate simulation of body waves. This is also reported by Xu et al. Xu et al. (1999) who also concluded that Rayleigh waves suffer more severely from numerical dispersion than body waves do. The Rayleigh wave generally exhibits a smaller wavelength in the vertical direction due to the exponential decay away from the surface. This may require significantly higher spatial sampling (Mittet, 2002). In our numerical tests we discovered that SSG and RSG simulations using higher order spatial operators across the free surface are stable but do not produce reasonable results. This is due to the poor accuracy of higher order operators when applied at discontinuities of the seismic

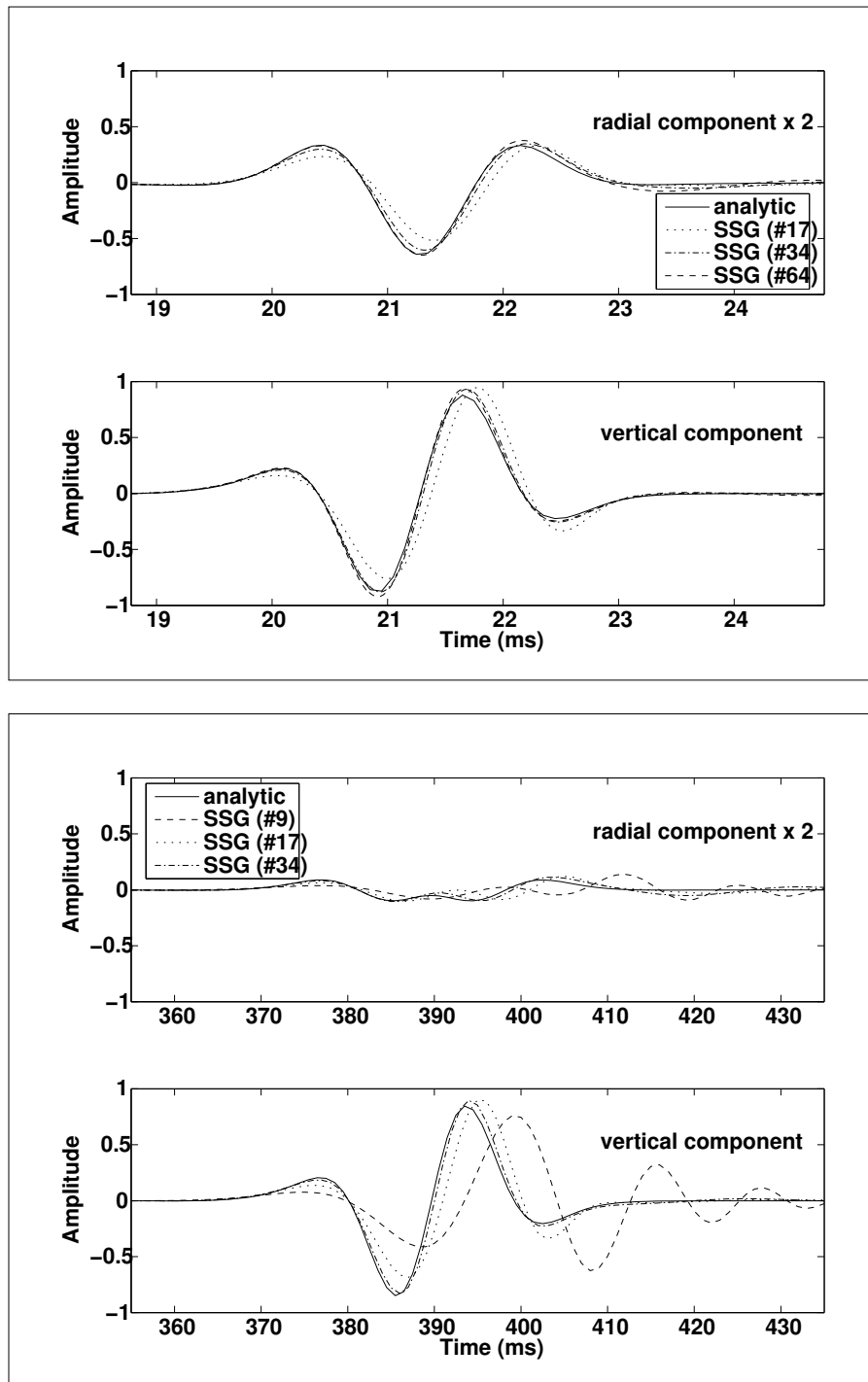


Figure 2: Seismograms for a planar free surface aligned with the grid. Offset is 60 m. a) hard rock and b) soft rock. SSG seismograms are compared with the analytical solution. Numbers denote the number of grid points per minimum wavelength used in the FD simulations.

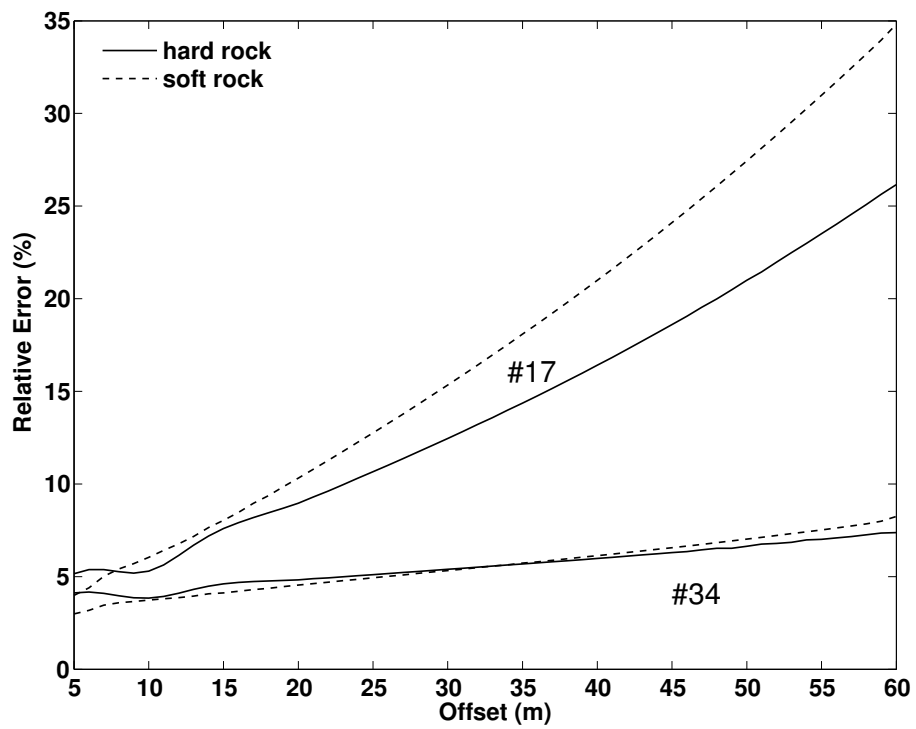


Figure 3: Relative errors (equation 3) as a function of offset for Rayleigh waves along a planar free surface aligned with the grid. Numbers denote grid points per minimum wavelength used in the simulations. Hard rocks and soft rocks show similar behaviour.

λ_{min}/dh	$dh(m)$	grid size	$dt(\mu s)$	time steps	run time on 8 CPUs (s)
<u>hard rock</u>					
17	0.2	500x400	20	2500	20
34	0.1	1000x800	10	5000	160
64	0.05	2000x1600	5	10000	1146
<u>soft rock</u>					
9	0.2	500x400	80	6250	45
17	0.1	1000x800	40	12500	360
34	0.05	2000x1600	20	25000	2800

Table 1: Discretization and run times for the hard rock and soft rock simulations. $\lambda_{min} = c_{min}/f_{max}$ denotes the minimum wavelength of the Rayleigh wave, dh is the spatial grid increment, and dt is the time step interval.

wavefield (Cunha, 1993).

Comparison with explicit boundary conditions

To facilitate a direct comparison of the performance of the heterogeneous and homogeneous approach we also apply explicit boundary conditions at the free surface. We choose two implementations. The first one is the classical so-called image method in which σ_{iy} ($i=x,z$) are imaged as odd functions across the free surface and σ_{yy} is explicitly set to zero (Levander, 1988; Robertsson, 1996; Gottschämer and Olsen, 2001). Particle velocity components are set to zero above the free surface (image method 3 discussed by Robertsson, 1996). The second implementation was more recently proposed by Mittet (2002). He suggested a simple ad hoc approach: set σ_{yy} and λ to zero on the free surface nodes, and set μ and ρ to half the internal value on the free surface nodes. Arithmetic averaging of the shear modulus is performed inside the earth. Mittet (2002) observed excellent agreement with the same analytical solution we use here.

Both implementations are tested using a 2nd-order SSG scheme (O(2,2)) and a 4th-order SSG scheme (O(2,4)). Seismograms obtained with the image method for the soft rock case are shown in Figure 4. A direct comparison with Figure 2b reveals that the overall accuracy of the image method is comparable to the heterogeneous approach. The image method applied in the O(2,2) SSG scheme simulates a Rayleigh wave that is slightly too slow (it arrives later – see Figure 4, top), whereas the Rayleigh wave is slightly too fast when 4th-order operators are used (Figure 4, bottom). 17 and 9 grid points per minimum wavelength for the 2nd-order and 4th-order simulations, respectively, seem to be sufficient for the image method to obtain good accuracy. The comparison of the performance of the image method (Figure 4, top) and the heterogeneous approach (Figure 2b) for 2nd-order FD operators leads to the conclusion that the heterogeneous approach requires roughly half the spatial sampling of the image method. The necessary sampling of the image method can be further reduced if higher order operators are used. If 4th-order operators are applied only 9 grid points are sufficient to obtain acceptable results. This is close to the rule-of-thumb for the necessary discretization with an O(2,4) SSG scheme to avoid numerical dispersion of body waves. The application of higher operators for heterogeneous free surface modelling is not possible.

The boundary condition of Mittet (2002) is less accurate (Figure 5) than the image method. The Rayleigh wave is significantly delayed even if the Rayleigh wave is discretized with more than 17 grid points per horizontal wavelength.

Dipping planar free surface

Now we test the accuracy of the heterogeneous approach for modeling Rayleigh wave propagation along a dipping planar interface. Differences in the simulations of dipping interfaces between the two numerical schemes are caused by two factors. First of all the two schemes differ in their directional variation of numerical dispersion Saenger et al. (2000). However, with decreasing grid increments (spatial grid size

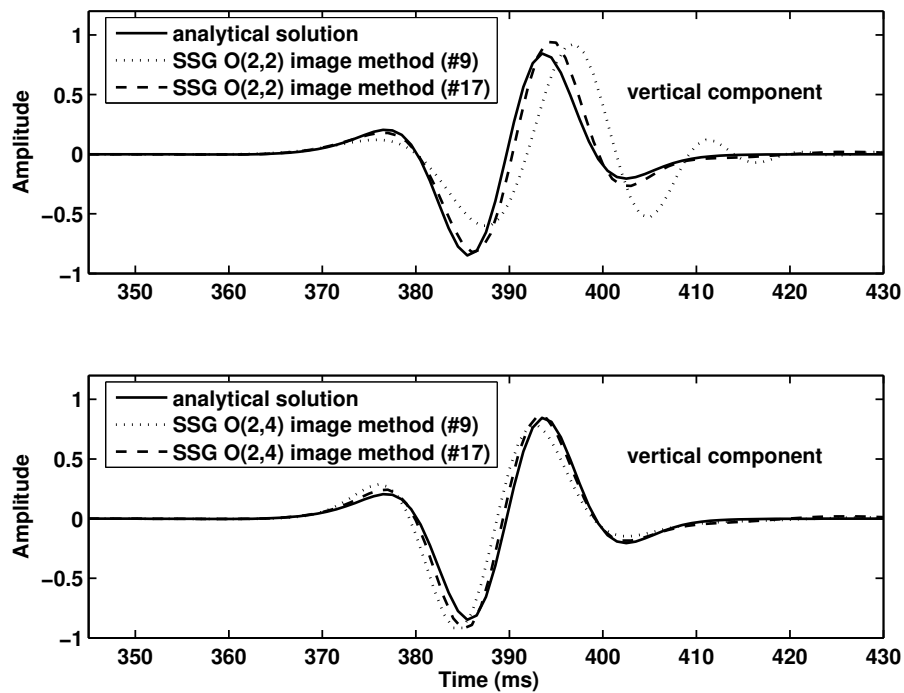


Figure 4: Explicit boundary condition (image method) applied at a planar free surface aligned with the grid. Offset is 60 m. Soft rock case. SSG scheme with 2nd-order spatial FD operators (O(2,2)) (top) and 4th-order operators (O(2,4)) (bottom) are used. FD seismograms (vertical components) obtained with 9 and 17 grid points per minimum Rayleigh wavelength are compared with the analytical solution.

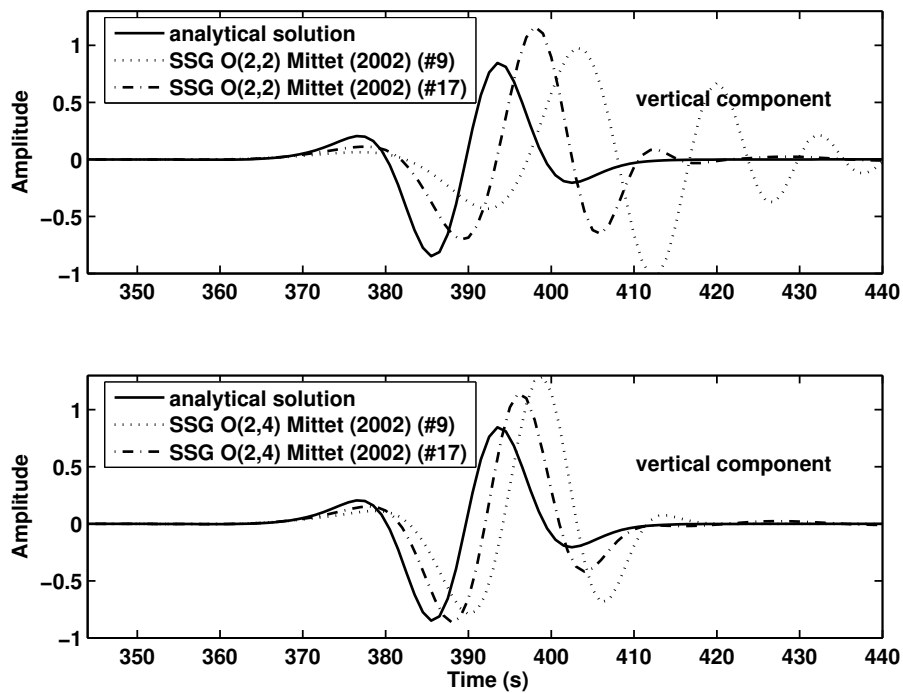


Figure 5: Explicit boundary condition proposed by Mittet (2002) applied at a planar free surface aligned with the grid. Offset is 60 m. Soft rock case. 2nd order (O(2,2)) and 4th order (O(2,4)) spatial FD operators are used. SSG seismograms with 9 and 17 grid points per minimum Rayleigh wavelengths are compared with the analytical solution.

and time step interval) this difference becomes less important. Secondly, differences are caused by the spatial discretization of the dipping interface which results in artificial steps (staircases) on the numerical grid. Due to the different spatial distributions of material parameters (Figure 1) and averaging procedures (equations 1 and 2) this leads to a different location of the effective free surface. We believe that most of the differences between the SSG and the RSG for dipping interfaces, which are described below, must be attributed to the different spatial representations of the effective free surfaces.

In the simulations of dipping free surfaces the receiver components are rotated into the directions parallel (radial) and perpendicular (vertical) to the orientation of the interface. Figure 6 shows seismograms of the vertical component calculated with the SSG and RSG for different dipping angles.

The corresponding errors (equation 3) are shown in Figure 7.

The direct P-wave (not shown) is modeled accurately even on coarser grids. Large errors, however, are observed for the Rayleigh wave which is shown in Figure 6. As expected, the best results are obtained when the free surface is aligned with the grid (0° and 90°). For dip angles away from 0° and 90° , the error increases and does so more rapidly for coarser grid spacings. Near the dip of 45° the error decreases. This is also reported by Vossen et al. (2002) for the SSG in case of a dipping fluid-solid boundary. The asymmetry of errors around 45° is related to different locations of the steps in the numerical interfaces.

If the free surface is not aligned with the grid, the Rayleigh wave is delayed and distorted in the results of both numerical schemes, but most severely for the SSG. Even for very fine grid spacings there remain substantial differences between the SSG and the analytical solution. For coarser grid spacings (17 points) the error is due to significant diffraction in the Rayleigh wave at irregular steps of the free surface. In the coarse grid RSG simulations edges of the free surface can lead to a "checker-board" pattern of the wavefield, i.e. alternating amplitudes between neighboring grid points. On finer grids, the SSG error is mainly due to the time delay of the Rayleigh wave. Note that the error of the SSG is still above 50 % around 45° dip angle (Figure 7b) even when 68 grids are used. The error of the RSG decreases much more rapidly with decreasing grid spacing. However, to achieve good accuracy for all dip angles ($E < 10\%$) a very fine sampling of the wavefield, more than approximately 60 grid points per minimum wavelength, is required.

CONCLUSIONS

In this work we investigated the accuracy of heterogeneous FD modeling of Rayleigh waves along planar free surfaces having different orientations with respect to the directions of the numerical grid. In the case of a planar free surface aligned with the grid the SSG and the RSG perform equally well, i.e. seismograms are almost identical. At least 15 to 30 grid points per minimum wavelength are needed to achieve good accuracy. This case, however, can be simulated on coarser grids with better accuracy and higher spatial FD operators using explicit boundary conditions, e.g. the image method.

Because of the simplicity of the heterogeneous approach the greatest application potential was expected for complex shaped free surfaces. In the case of dipping planar free surfaces, however, accuracy decreases. The error increases significantly for dipping angles away from 0° . Errors are most severe for the SSG: even when using 68 grid points per minimum wavelength a significant effect of the slope of the free surface is observed. Good results can be obtained with the RSG for all dipping angles if more than approximately 60 grid points per minimum wavelength are used. The required dense spatial sampling, however, leads to extremely high computational requirements especially for realistic 3-D scenarios. Variable grid FD modeling using small grid spacing near free surfaces and coarser grid spacing in the interior of the earth thus seems to be a necessary implementation to apply heterogeneous free surface modeling for routine applications. The implementation of explicit boundary conditions for tilted surfaces is another way to reduce the necessary sampling close to free surfaces.

ACKNOWLEDGMENTS

We thank Jose Carcione (assistant editor) for making available the code for calculation the analytical solution and his comments. The simulations were performed on the parallel supercomputers at Kiel University and on the HLRN system (Berlin and Hannover).

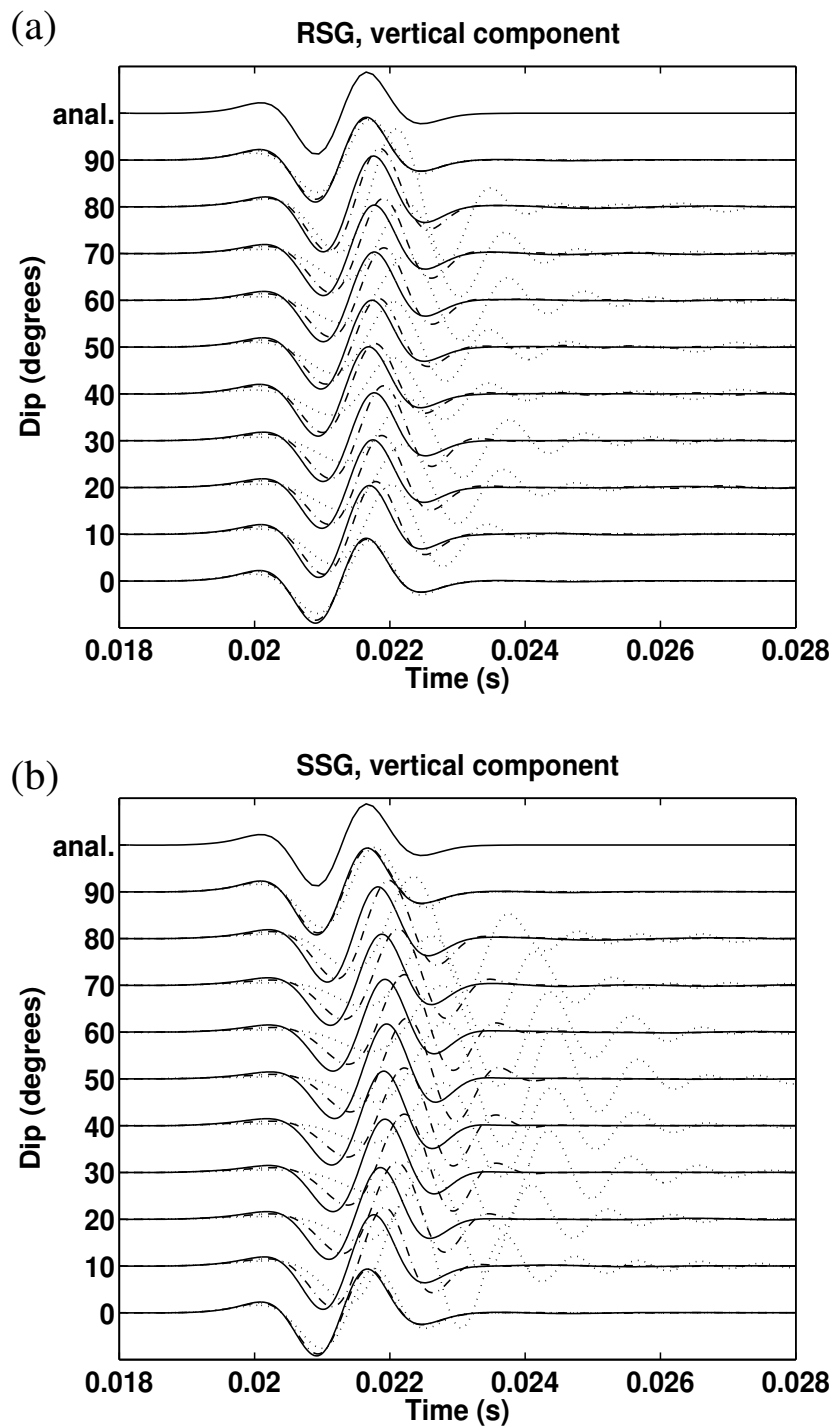


Figure 6: FD seismograms (vertical component) at 60 m offset for different dipping angles of the free surface. 68 (solid), 34 (dashed-dotted), and 17 (dotted) grid points per minimum wavelength were used in the simulations. (a) RSG scheme and (b) SSG scheme. The analytical solution is shown in the top level trace of each section.

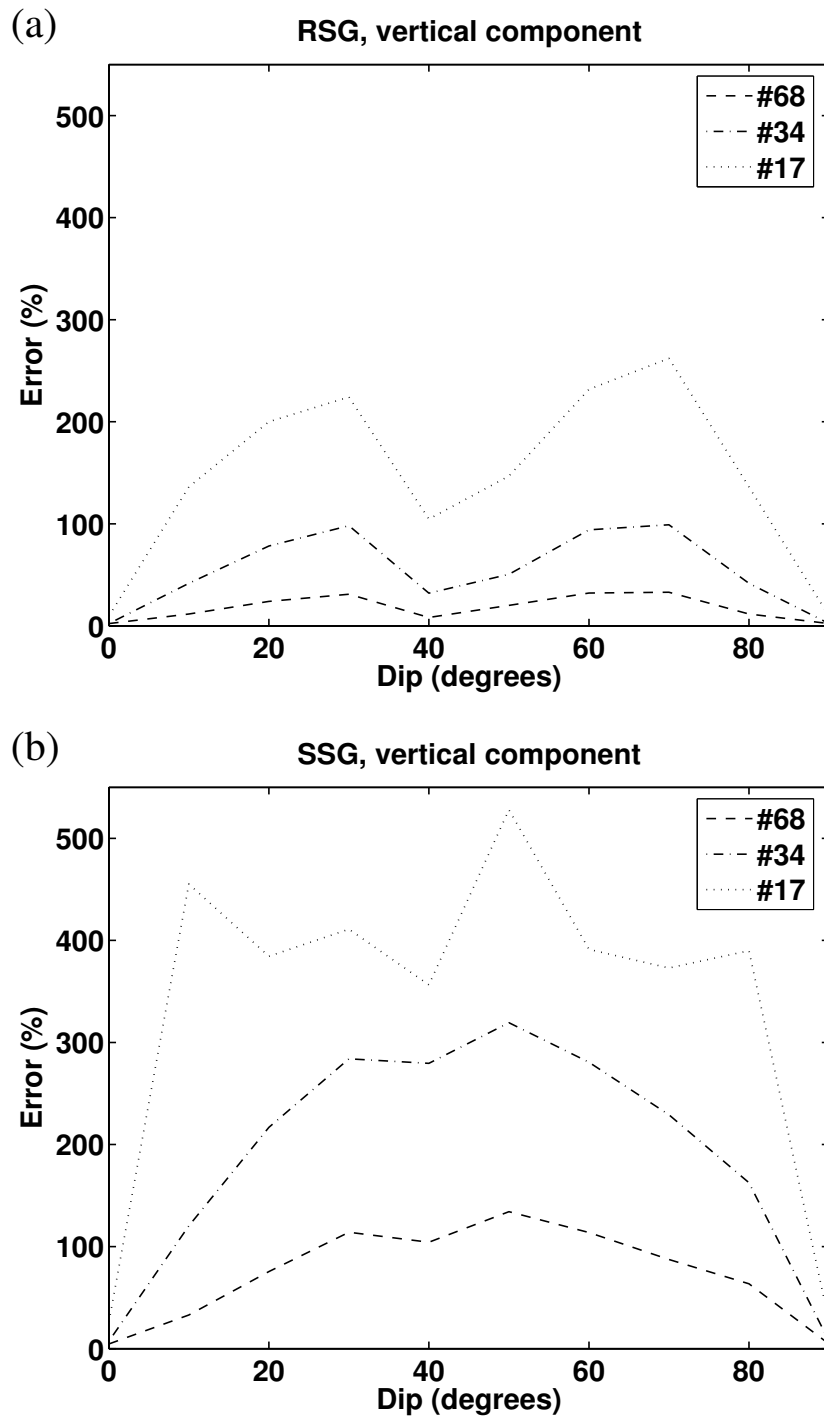


Figure 7: Error of seismograms shown in Figure 6. (a) RSG scheme and (b) SSG scheme. Errors of simulations with 68, 34, and 17 grid points per minimum wavelength are compared.

REFERENCES

- Berg, P., If, F., Nielsen, P., and Skovgaard, O. (1994). *Analytical reference solutions*, pages 421–427. Pergamon Press.
- Blanch, J., Robertsson, J., and Symes, W. (1995). Modeling of a constant Q: Methodology and algorithm for an efficient and optimally inexpensive viscoelastic technique. *Geophysics*, 60(1):176–184.
- Bohlen, T. (2002). Parallel 3-D viscoelastic finite-difference seismic modelling. *Comput. and Geosci.*, 28(8):887–899.
- Boore, D. (1972). Finite-difference methods for seismic wave propagation in heterogeneous materials. In Bolt, B., editor, *Methods of computational physics*, volume 2. Academic Press, New York.
- Cunha, C. A. (1993). Elastic modeling in discontinuous media. *Geophysics*, 59(12):1840–1851.
- Falk, J. (1998). *Efficient Seismic Modeling of Small-Scale Inhomogeneities by the Finite-Difference Method*. PhD thesis, University of Hamburg.
- Fellinger, P., Marklein, R., K.J., L., and Klaholz, S. (1995). Numerical modeling of elastic wave propagation and scattering with efit - elastodynamic finite integration technique. *Wave Motion*, 21:47–66.
- Fornberg, B. (1988). The pseudospectral method: Accurate representation of interfaces in elastic wave calculations. *Geophysics*, 53:625 – 637.
- Frankel, A. and Leith, W. (1992). Evaluation of topographic effects on p- and s-waves of explosions at the northern novaya zemiya test site using 3-D numerical simulations. *Geophys. Res. Lett.*, 19:1887–1890.
- Gold, N., Shapiro, S. A., and Burr, E. (1997). Modelling of high contrasts in elastic media using a modified finite difference scheme. In *68th Ann. Internat. Mtg., Soc. Expl. Geophys., Expanded Abstracts*, volume 97, page ST 14.6.
- Gottschämer, E. and Olsen, K. (2001). Accuracy of the explicit planar free-surface boundary condition implemented in a fourth-order staggered-grid velocity-stress finite-difference scheme. *Bull., Seis Soc. Am.*, 91(3):617–623.
- Graves, R. (1996). Simulating seismic wave propagation in 3D elastic media using staggered-grid finite differences. *Bull., Seis Soc. Am.*, 86(4):1091–1106.
- Hayashi, K., Burns, D. R., and Toksöz, M. N. (2001). Discontinuous-grid finite-difference seismic modeling including surface topography. *Bull., Seis Soc. Am.*, 91(6):1750–1764.
- Hestholm, S. O. (2003). Elastic wave modeling with free surfaces: stability of long simulations. *Geophysics*, 68(1):314–321.
- Hestholm, S. O. and Ruud, B. O. (1998). 3-D finite-difference elastic wave modeling including surface topography. *Geophysics*, 63:613–622.
- Imhof, M. G. (2003). Calculating the seismic effect of 3-D underground structures and topography with the finite-difference method. In *74th Ann. Internat. Mtg., Soc. Expl. Geophys., Expanded Abstracts*, pages 1939–1942. Soc. Expl. Geophys.
- Jih, R., K. L. McLaughlin, K., and d. Z. A (1988). Free-boundary conditions of arbitrary polygonal topography in a two-dimensional explicit elastic finite-difference scheme. *Geophysics*, 53:1045 – 1055.
- Kelly, K., Ward, R., Treitel, S., and Alford, R. (1976). Synthetic seismograms: A finite-difference approach. *Geophysics*, 41(1):2–27.
- Krüger, O. S., Saenger, E. H., and Shapiro, S. (2005). Scattering and diffraction by a single crack: an accuracy analysis of the rotated staggered grid. *Geophysical J. Internat.*, 162:25–31.

- Levander, A. (1988). Fourth-order finite-difference P-SV seismograms. *Geophysics*, 53(11):1425–1436.
- Mittet, R. (2002). Free-surface boundary conditions for elastic staggered-grid modeling schemes. *Geophysics*, 67(5):1616–1623.
- Moczo, P., Kristek, J., Vavrycuk, V., Archuleta, R., and Halada, L. (2002). Heterogeneous staggered-grid finite-difference modeling of seismic motion with volume harmonic and arithmetic averaging of elastic moduli and densities. *Bull., Seis Soc. Am.*, 92(8):3042–3066.
- Ohminato, T. and Chouet, B. (1997). A free-surface boundary condition for including 3d topography in the finite-difference method. *Bull., Seis Soc. Am.*, 87(2):494–515.
- Opršal, I. and Zahradník, J. (1999). Elastic finite-difference method for irregular grids. *Geophysics*, 64:240–250.
- Robertsson, J., Blanch, J., and Symes, W. (1994). Viscoelastic finite-difference modeling. *Geophysics*, 59(9):1444–1456.
- Robertsson, J. and Holliger, K. (1997). Modeling of seismic wave propagation near the earth's surface. *Phys. Earth Plan. Int.*, 104:193–211.
- Robertsson, J. O. A. (1996). A numerical free-surface condition for elastic/viscoelastic finite-difference modeling in the presence of topography. *Geophysics*, 61:1921–1934.
- Saenger, E. and Bohlen, T. (2004). Finite-difference modeling of viscoelastic and anisotropic wave propagation using the rotated staggered grid. *Geophysics*, 69(2):583–591.
- Saenger, E., Gold, N., and Shapiro, S. (2000). Modeling the propagation of elastic waves using a modified finite-difference grid. *Wave Motion*, 31(1):77–92.
- Tessmer, E. and Kosloff, D. (1994). 3-d elastic modeling with surface topography by a chebyshev spectral method. *Geophysics*, 59:464–473.
- Virieux, J. (1986). P-SV wave propagation in heterogeneous media: velocity-stress finite-difference method. *Geophysics*, 51(4):889–901.
- Vossen, R., Robertsson, J., and Chapman, C. (2002). Finite-difference modeling of wave propagation in a fluid-solid configuration. *Geophysics*, 67(2):618–624.
- Xu, H., Day, S. M., and Minster, J.-B. (1999). Two-dimensional linear and nonlinear wave propagation in a half-space. *Bull., Seis Soc. Am.*, 89(4):903–917.
- Zahradník, J., Moczo, P., and Hron, F. (1993). Testing four elastic finite difference schemes for behaviour at discontinuities. *Bull., Seis Soc. Am.*, 83:107–129.
- Zahradník, J. and Priolo, E. (1999). Heterogeneous formulations of elastodynamic equations and finite-difference schemes. *Geophysical J. Internat.*, 120:663–676.
- Zahradník, J. and Urban, L. (1984). Effect of a simple mountain range on underground seismic motion. *Geophys. J. R. astr. Soc.*, 79:167–183.